Supporting Information for

Photoinduced electron transfer from PbS quantum dots to cobalt(III) Schiff base complexes: light activation of a protein inhibitor

Mark D. Peterson[‡£], Robert J. Holbrook[‡†£], Thomas J. Meade*[†£], and Emily A. Weiss*[£]

[£]*Department of Chemistry, Northwestern University, 2145 Sheridan Rd., Evanston, IL 60208-3113*

[†]*Department of Molecular Biosciences, 2205 Tech Drive, Hogan 2100, Evanston, IL 60208, Department of Neurobiology, 2205 Tech Drive, Hogan 2100, Evanston, IL 60208, and Department of Radiology, Feinberg School of Medicine, Northwestern University, 676 N. St. Clair St., Chicago, IL 60611*

*Corresponding authors. Email: e-weiss@northwestern.edu, tmeade@northwestern.edu

EXPERIMENTAL METHODS

Synthesis of Colloidal PbS QDs. We synthesized PbS quantum dots (QDs) using a procedure adapted from that of Hines and Scholes.[1] We deaerated a solution containing 2.0 mL oleic acid (OA) and 18.0 mL 1-octadecene (ODE) in a 50 mL three-neck round bottom flask at room temperature by bubbling with nitrogen gas for 30 minutes. We subsequently added 0.36 g PbO and heated the solution to 150 °C under nitrogen while stirring until the solution turned clear, then cooled the solution to 110 °C. To initiate growth of QDs we injected 0.17 mL hexamethyldisilathiane dissolved in 8 mL ODE, and allowed the dots to grow for ~10 minutes. After cooling the reaction to room temperature we washed the QDs twice with 50 mL methanol, then centrifuged a 1:1 (v/v) mixture of QD:acetone at 5000 rpm for 5 minutes to produce a dark pellet. The pellet was re-dispersed in acetone, centrifuged, dried, and finally dissolved in $CHCl_3$ to produce our stock solution.

Synthesis of Cobalt Schiff Bases. The complex, $[Co(acacen)(Im)_2]Br$, was synthesized according to previously reported procedures.[2] The alkylcarboxylate functionalized Co-SB complex discussed below, $[Co(III)(heptanoic\ acido)(acacen)(NH_3)_2]Cl$, was also synthesized according to previously reported procedures.[3]

Preparation of PbS QD/Co(III)-SB Mixtures. To prepare the Co(III)-SB/PbS QD samples, we transferred a methonolic solution of the Co(III)-SB into a scintillation vial and evaporated to dryness under nitrogen before adding 1.4×10^{-5} M PbS QDs in $CHCl_3$. The vial was shaken until the Co(III)-SB complex was dissolved, and the solution was allowed to equilibrate for 24 hours before performing measurements.

Ground State Absorption. We performed ground state absorption measurements, Figure S1, on a Varian Cary 5000 using 2-mm quartz cuvettes. Spectra were baseline corrected by subtracting the absorption spectrum of chloroform.

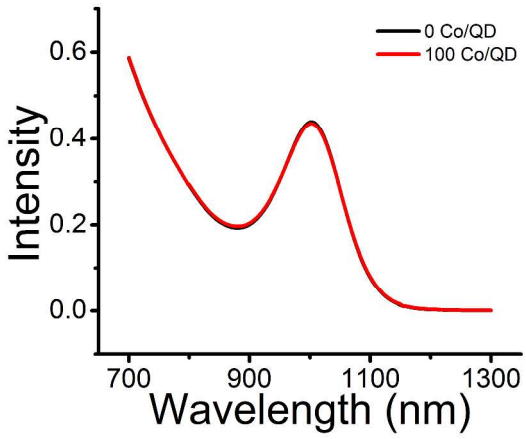

Figure S1. Ground state absorption spectra of 1.4×10^{-5} M PbS QDs in $CHCl_3$ with (red) and without (black) 100 Co(III)-SB added per QD in a 2-mm quartz cuvette.

Photoluminescence (PL). We prepared samples for photoluminescence by injecting a known volume of the Co(III)-SB in methanol into a small, clean scintillation vial and

evaporating the solvent under nitrogen before adding 3 mL 1.4×10^{-5} M PbS QDs in $CHCl_3$. We gently shook the vial until the residue left by the SB was dissolved, and allowed the solution to equilibrate for 24 hours before collecting PL spectra. PL spectra were collected at an optical density of 0.83 at the band edge on a Horiba Fluorolog-3 spectrofluorometer in the right-angle geometry using 1-cm quartz cuvettes. The excitation and emission slit widths were set to 3 nm. We pumped the solution at 850 nm, and divided the measured intensity by the instantaneous intensity of the excitation source at all wavelengths.

Transient Absorption (TA). We used a commercial EOS spectrometer, which is described in detail elsewhere,[4] for NIR TA experiments. We prepared samples for TA by placing 800 μL of the samples used for PL measurements into 2-mm quartz cuvettes with a teflon stir bar. We pumped the solutions at 850 nm under constant stirring to avoid local heating and charge buildup, and collected spectra at 1 kHz for ~1 hr.

NMR. NMR spectra were obtained on a Bruker 600 MHz Avance III NMR spectrometer with a variable temperature unit. We calculated the relative abundance of Co-Im and Co-4MeIm bond formation by integrating the ^{1}H NMR chemical shifts, reported in ppm, with respect to the internal reference, tetramethylsilane. In order to follow the formation of Co-Im and Co-4MeIm bonds in solution, the ^{1}H aromatic signal of the 4-position protons of Im in Co-Im (6.52-6.62 ppm) and the 5-position protons of 4MeIm in Co-4MeIm (6.15-6.25 ppm) were integrated; integrations are calibrated with respect to the ethylene protons of the oleic acid ligands of the QD (5.28-5.40 ppm). Figure S2 shows the decay of the Co-Im peak and growth of the Co-4MeIm peak in time for samples in the dark and under illumination. The faster decay of the Co-Im peak, and corresponding growth of the Co-4MeIm peak, under illumination illustrates the increased ligand reactivity upon irradiation of the QD.

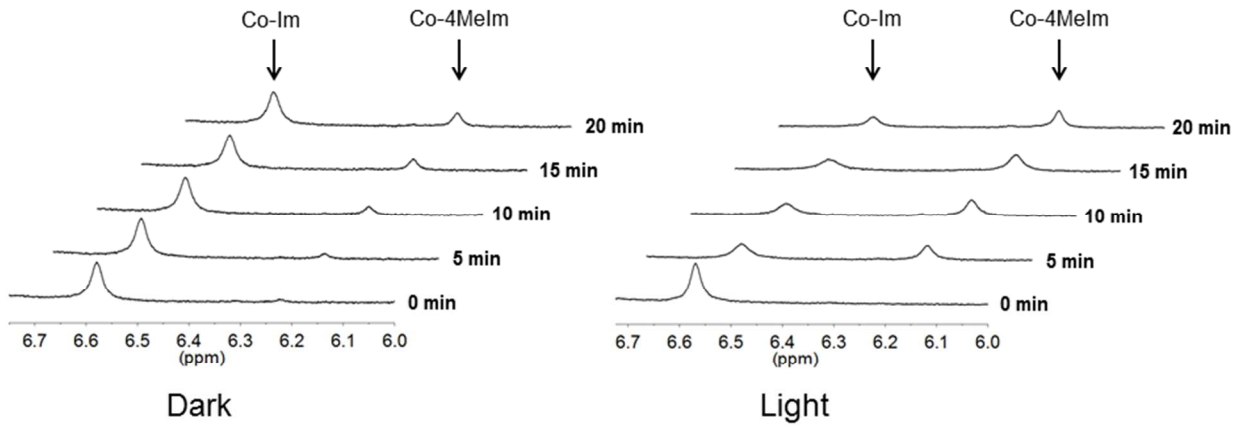

Figure S2. Time dependent NMR spectra showing the change in Co-Im and Co-4MeIm peaks in the dark ("Dark") and upon illumination ("Light") with a halogen lamp passed through a 400-nm long pass filter. The faster decay of the Co-Im peak, and corresponding growth of the Co-4MeIm peak, under illumination illustrates the increased ligand reactivity upon irradiation of the QD.

Formulation and Justification for Eq. 1. As described in the main text, the observed rate constant for charge transfer in systems comprising QDs and a redox active adsorbate is linearly proportional to the number of adsorbates bound per QD.[5-7] Therefore, the model used in fitting the TA data must account for the distribution in rate constants by describing each subpopulation of QDs with m quenchers, where m = 0, 1, 2, ..., N and N is the total number of binding sites (empty and filled by native ligands). This situation can be described by eq. S1, where OD is the optical density and A_m is the

$$\Delta OD = \sum_{m=0}^{N} A_m e^{-mk_{\text{int}}t} \qquad \text{(S1)}$$

amplitude of each exponential component that decays in time t with an intrinsic rate constant of k_{int}. The normalized amplitudes represent the fractional contribution of each subpopulation to the total ensemble, and are therefore binomially distributed,[8,9] as shown in eq. S2, where θ is the

$$A_m = \binom{N}{m}(\theta)^m(1-\theta)^{N-m} \qquad \text{(S2)}$$

mean fractional surface coverage of adsorbates on the QD. Substituting eq. S2 into eq. S1 yields eq. S3, which allows us to model the change in optical density resulting from charge transfer for the entire ensemble as a function of only the intrinsic rate constant. The complete fitting function

$$\Delta OD = (1 + (e^{-k_{\text{int}}t} - 1)\theta)^N \qquad \text{(S3)}$$

includes terms to account for the instrument response function and charge recombination, as shown in the main text.

Surface Coverage of Co-SB on the QD. The Co(III)-SB/QD system is modeled with two binomial distributions:[5] one to describe the average number of available adsorption sites per QD, η (a quantity that depends on surface chemistry and size of the QD), and one to describe the probability of finding a QD within the ensemble with *m* adsorbed Co(III)-SB molecules, given the distribution in the number of available sites. The probability of finding a QD with *m* adsorbed Co-SB molecules given *N* mean total surface sites per QD, η mean available surface sites per QD, and a mean fractional surface coverage of Co-SB of θ, is given by eq. S4.[8,9]

$$P(m \mid N, \theta_a, \eta) = \sum_{n=0}^{N}\left[\binom{N}{n}\binom{\eta}{N}^n\left(1-\frac{\eta}{N}\right)^{N-n}\right]\left[\binom{n}{m}\theta^m(1-\theta)^{n-m}\right] \qquad \text{(S4)}$$

If we assume that electron transfer occurs within each QD/Co(III)-SB complex with at least one Co(III)-SB adsorbed in an electron transfer-active geometry, then the ratio PL/PL_0 equals the fraction of the QD sample with zero adsorbed Co(III)-SB molecules, $P(0|N,\theta,\eta)$. For $m = 0$, the binomial distribution describing the number of adsorbates per QD reduces to $PL/PL_0 = (1-\theta)^N$.

Using an estimate of $N = 282$ for this size of QD, and the measured value of PL/PL_0 for each concentration of added Co-SB (Figure 1B), we calculate θ at each quencher concentration.

We can find the adsorption constant of the QD/Co(III)-SB redox couple by plotting θ against the concentration of free quencher in solution. We find the concentration of free ligand by subtracting the number of Co(III)-SBs bound to QDs from the total number of added Co(III)-SBs, and converting to concentrations, $[Co\text{-}SB]_{free} = [Co\text{-}SB]_{total} - N\theta[QDs]$. Fitting a plot of θ *versus* the free quencher concentration to a Langmuir isotherm, as shown in eq. S5, returns the

$$\theta = \theta_{\max} \frac{K_a[Co-SB]_{free}}{1 + K_a[Co-SB]_{free}} \qquad \text{(S5)}$$

maximum (saturated) surface coverage of Co(III)-SB on the QD surface, $\theta_{\max}$, and the equilibrium binding contant for the QD/Co(III)-SB system for this particular concentration of QDs, as shown in Figure S3.[9] The fit values for θ_{max} and K_a are 0.87% and 1.1×10^{-3} M^{-1}, respectively.

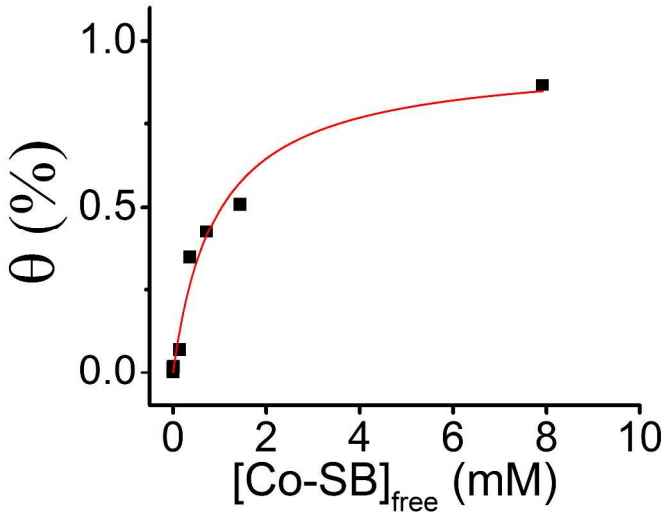

Figure S3. Plot of the mean fractional surface coverage of 1.4×10^{-5} M PbS QDs in $CHCl_3$ against the concentration of free Co(acacen)$(Im)_2$ in solution, and fit to a Langmuir isotherm as shown in eq. S5.

Intrinsic Electron Transfer Rate for [Co(III)(Heptanoic Acido)(Acacen)$(NH_3)_2$]Cl. In addition to the Co(III)-SB used in the main text, we investigated a tightly binding alkylcarboxylate functionalized Co(III)-SB as shown in Chart S1. The carboxylic acid group of this molecule provides a means for strong electronic coupling to the Pb^{2+} surface atoms in PbS QDs. We measured the decay of the band-edge bleach in samples comprising 1.4×10^{-5} M PbS QDs in $CHCl_3$ and 1.4×10^{-3} M Co(III)(heptanoic acid)(acacen)$(NH_3)_2$, as shown in Figure S4, and fit to eq. 1 in the main text to obtain an intrinsic electron transfer rate of 2.2 ns – about two orders of magnitude faster than we observed for the same QDs with Co(III)(acacen)$(Im)_2$. This experiment demonstrates that creation of a chemisorbed linkage between the QD and the Co(III)-SB is a good strategy for increasing PET yield in these systems, if necessary.

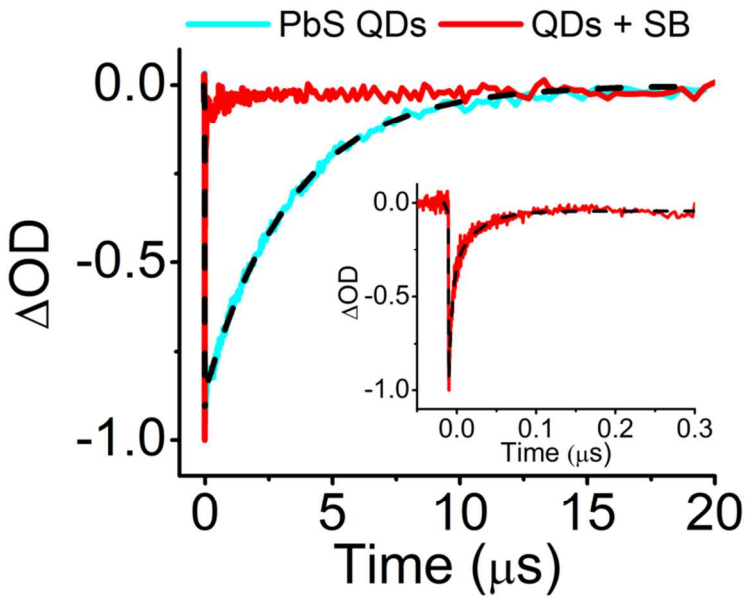

Figure S4. TA kinetics of PbS QDs (blue) and QDs with the alkylcarboxylated Co(III)-SB ("QDs + SB", red) with fits (dashed black lines) to a sum of exponential functions convoluted with an instrument response function, eq 1. The traces reflecting samples containing the Co(III)-SB are plotted on a smaller scale in the inset, and return an intrinsic electron transfer time of 2.2 ns.

Chart S1. An alkylcarboxylate functionalized Co-SB.

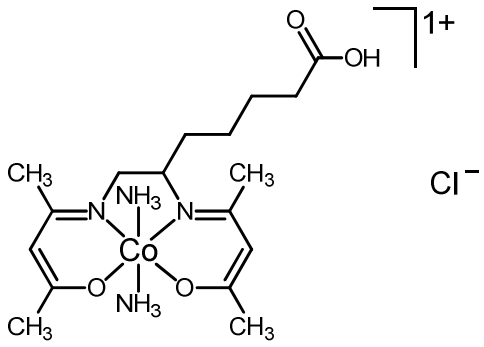

The presence of Co(III) is necessary to quench the PL of the QDs. We can rule out charge transfer from PbS QDs to imidazole within the Co(III)-SB complex based on the respective energy levels of PbS QDs[10,11] and imidazole.[12,13] To show that PbS QDs cannot donate an

electron or hole to acacen, we prepared PbS QD/acacen solutions in concentrations similar to those in the main text. Figure S5 shows that the PL of PbS QDs does not quench upon addition of these organic molecules, where the legend denotes the number of quenchers per QD (QDs are 1.4×10^{-5} M). The inability of acacen to quench the PL of PbS suggests that acacen does not accept a charge from these QDs, and does not disrupt the surface structure by creating trap sites. The only portion of the Co(acacen)$(Im)_2$ complex available for electron transfer is therefore the Co, which undergoes axial ligand removal upon photoexcitation of the PbS QD, consistent with electron transfer.

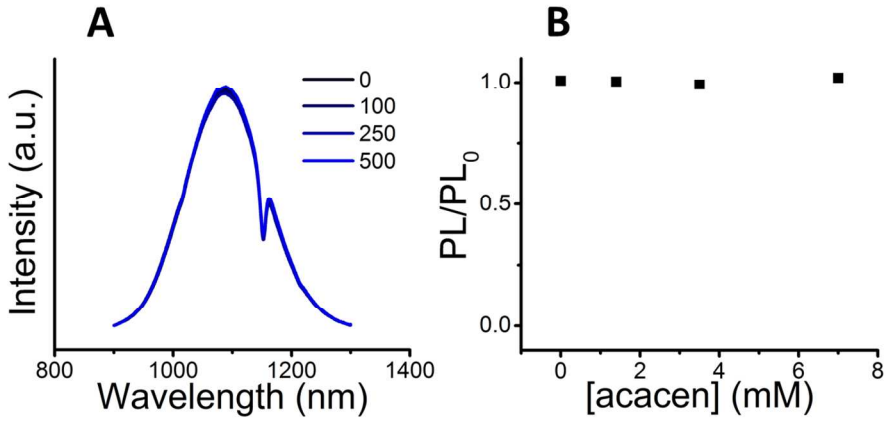

Figure S5. (A) PL spectra of acacen on 1.4×10^{-5} M PbS QDs. The inability of acacen to quench the PL suggests that it cannot accept a charge from the PbS QD, and does not create trap sites that extinguish luminescence. The legend indicates the number of acacen added to solution per QD. (B) PL/PL_0 for the solutions shown in A.

A change in the reduction potential of the Co(III) center changes the electron transfer rate. We performed further experiments in which we prepared PbS QDs with a Co(III)-SB identical to that used in the main text with the exception that the axial Im ligands were replaced with N-methylimiazole (NMeIm). The reduction potential of the Co(III)-SB with NMeIm ligands is 100 meV higher than the corresponding complex with Im,[14] and should therefore undergo

electron transfer at a slower rate. We expect this slower rate to manifest as inferior PL quenching and a reduced rate of bleach decay in the TA spectra. Figure S6 shows that the magnitude of PL quenching in solutions containing Co(acacen)(NMeIm)$_2$ is reduced compared to Co(acacen)(Im)$_2$, consistent with electron transfer. Figure S7 shows that the rate of the bleach decay is also reduced, as expected.

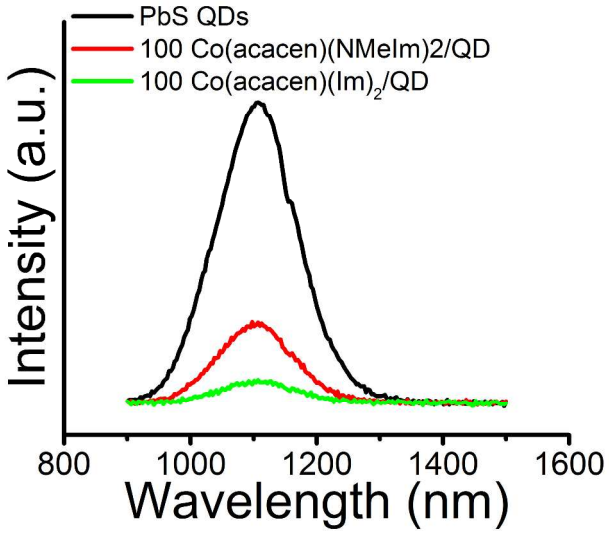

Figure S6. PL intensity of 1.4x10^{-5} M PbS QDs without Co(III)-SB (black), with 100 Co(acacen)(NMeIm)$_2$ added per QD (red), and with 100 Co(acacen)(Im)$_2$ added per QD, (green). The inferior quenching ability of Co(III)-SB with NMeIm rather than Im as the axial ligand is consistent with electron transfer.

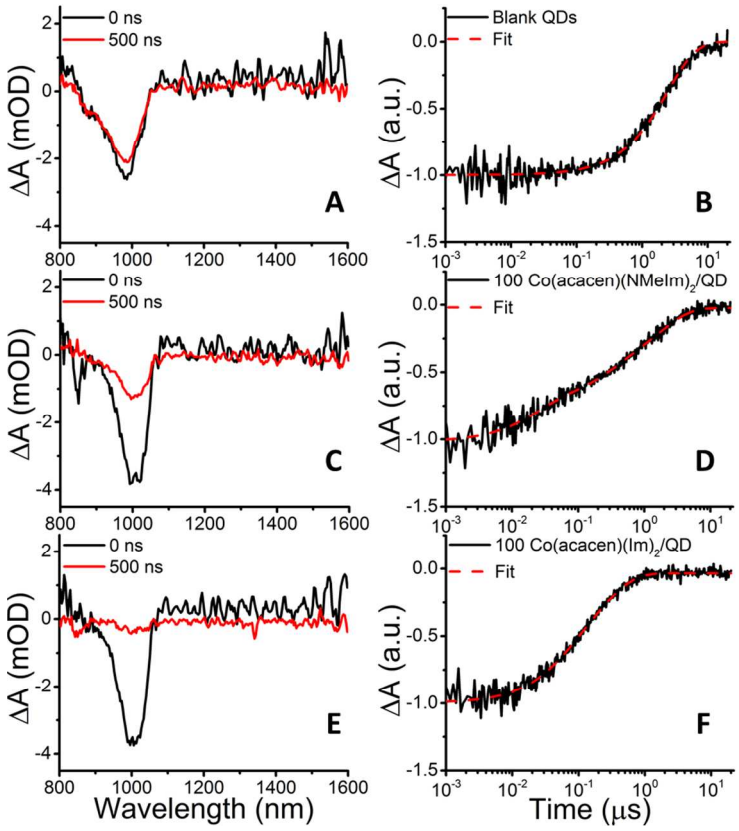

Figure S7. TA spectra of 1.4×10^{-5} M PbS QDs without Co(III)-SB (A), with 100 equivalents of $Co(acacen)(NMeIm)_2$ (C), and with 100 equivalents of $Co(acacen)(Im)_2$ (E), showing the magnitude of the band-edge bleach immediately after excitation ("0 ns", black) and 500 ns after excitation ("500 ns", red). The decay of the bleach in time is shown for the same samples in figures (B), (D), and (F), respectively. Compared to samples in which the Co(III)-SB has Im as the axial ligand, we observe a slower decay of the bleach with NMeIm, though both samples accelerate the decay with respect to the blank, as expected for electron transfer.

Charge Transfer is not Diffusion-Limited. Systems in which electron transfer is diffusion limited follow the well-known Stern-Volmer relationship, as shown in eq. S6, where PL_0 is the

$$\frac{PL_0}{PL} = 1 + K[Q] \qquad \text{(S6)}$$

photoluminescence intensity of a sample without a quencher, *PL* is the photoluminescence intensity of a sample containing quencher at concentration *[Q]*, and *K* is the quenching constant. We demonstrate that electron transfer in the QD/Co(III)(acacen)$(Im)_2$ system is not diffusion limited by showing that the relationship between PL_0/PL and quencher concentration is not linear, as shown in Figure S8. The data fits well to a relationship derived by assuming a binomial distribution of quenchers adsorbed to the surfaces of QDs.[9]

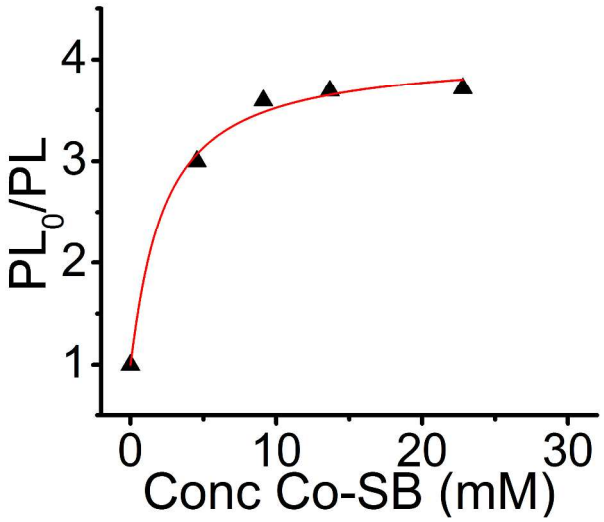

Figure S8. Plot of PL_0/PL verses the concentration of quencher molecules for 1.4×10^{-5} M PbS QDs in $CHCl_3$ with varying concentrations of Co(acacen)$(Im)_2$. The data are clearly nonlinear, and are fit to an equation derived by assuming a binomial distribution of quenchers adsorbed to the surfaces of QDs, as discussed in ref 9.

Fitting Parameters for the Electron Transfer Rate Equation. Figure 3D in the main text shows kinetic traces reflecting electron transfer from PbS QDs to Co(acacen)$(Im)_2$, along with fits to eq. 1. Table S1 summarizes the fit parameters for charge transfer and recombination, where θ and N are held fixed.

Table S1. A summary of the parameters for the fits shown in Figure 3D in the main text.

A_{eT}	$\tau_{int} = 1/k_{eT,int}$ (ns)	A_{CR}	$\tau_{CR} = k_{CR}$ (ns)	θ	N
0.52	125	0.48	258	0.0102	272

REFERENCES

(1) Hines, M. A.; Scholes, G. D. *Adv. Mater.* **2003**, *15*, 1844.

(2) Manus, L. M.; Holbrook, R. J.; Atesin, T. A.; Heffern, M. C.; Harney, A. S.; Eckermann, A. L.; Meade, T. J. *Inorg. Chem.* **2013**, *52*, 1069.

(3) Hurtado, R. R.; Harney, A. S.; Heffern, M. C.; Holbrook, R. J.; Holmgren, R. A.; Meade, T. J. *Mol. Pharm.* **2012**, *9*, 325.

(4) McArthur, E. A.; Morris-Cohen, A. J.; Knowles, K. E.; Weiss, E. A. *J. Phys. Chem. B* **2010**, *114*, 14514.

(5) Morris-Cohen, A. J.; Frederick, M. T.; Cass, L. C.; Weiss, E. A. *J. Am. Chem. Soc.* **2011**, *133*, 10146.

(6) Song, N.; Zhu, H.; Jin, S.; Zhan, W.; Lian, T. *ACS Nano* **2010**, *5*, 613.

(7) Rodgers, M. A. J.; Da Silva E Wheeler, M. F. *Chem. Phys. Lett.* **1978**, *53*, 165.

(8) Tachiya, M. *Chem. Phys. Lett.* **1975**, *33*, 289.

(9) Morris-Cohen, A. J.; Vasilenko, V.; Amin, V. A.; Reuter, M. G.; Weiss, E. A. *ACS Nano* **2011**, *6*, 557.

(10) Jasieniak, J.; Califano, M.; Watkins, S. E. *ACS Nano* **2011**, *5*, 5888.

(11) Hyun, B.-R.; Zhong, Y.-W.; Bartnik, A. C.; Sun, L.; Abruña, H. D.; Wise, F. W.; Goodreau, J. D.; Matthews, J. R.; Leslie, T. M.; Borrelli, N. F. *ACS Nano* **2008**, *2*, 2206.

(12) Jagoda-Cwiklik, B.; Slavic□ek, P.; Cwiklik, L.; Nolting, D.; Winter, B.; Jungwirth, P. *J. Phys. Chem. A* **2008**, *112*, 3499.

(13) Wang, H. L.; O'Malley, R. M.; Fernandez, J. E. *Macromolecules* **1994**, *27*, 893.

(14) Böttcher, A.; Takeuchi, T.; Hardcastle, K. I.; Meade, T. J.; Gray, H. B.; Cwikel, D.; Kapon, M.; Dori, Z. *Inorg. Chem.* **1997**, *36*, 2498.